Theoretical Studies in Epitaxial Stabilization of ZnO-based Light-emitting Semiconductors

Po-Liang Liu[1*], Yu-Jin Siao[1], and Ming-Hsien Lee[2]

[1] Graduate Institute of Precision Engineering, National Chung Hsing University, Taichung, Taiwan 402, Republic of China

[2] Department of Physics, Tamkang University, Tamsui, Taipei, Taiwan 251, Republic of China
E-mail addresses: pliu@dragon.nchu.edu.tw

ABSTRACT

We present first-principle calculations on the strained $Zn_{1-x}(Be,Mg,Al)_xO$ alloy systems. The epitaxial softening of (0001)-oriented $Zn_{1-x}(Be,Mg,Al)_xO$ strained layer lattices are investigated, and the ZnO strained layers could be stabilized with adding the aluminium compositions. A detailed analysis of the preferred (epitaxial) orientation of ZnO strained layer superlattices is examined, and $<2\bar{1}\bar{1}0>$-oriented ZnO is more stable than (0001)- or $(10\bar{1}0)$-oriented ZnO. Using the harmonic elasticity theory, we find the $q_{harm}([0001])$ is the highest and the $q_{harm}([2\bar{1}\bar{1}0])$ is much softer than <0001> or $<10\bar{1}0>$. In addition, the slightly softening of $<11\bar{2}l>$ in $Zn_{1-x}(Be,Mg,Al)_xO$ strained layer lattices is observed. The findings agree with previously reported experimental results.

Keywords: LED, ZnO, first-principle calculation, epitaxy.

I. INTRODUCTION

The device quality ZnO films are expected to next generation materials applied in the field of photo-electronic devices. It is partly due to the widely tunable lattice constant for being a new class of templates and partly due to the direct tunable bandgaps. Thus, they have the potential to develop inexpensive lasers and nanophotonics covered a wide wavelengths range in the blue, green and UV lighting. Light-emitting semiconductor devices rely on materials that possess single-crystal epilayers due to high quality intrinsic epilayers having high carrier mobility and low residual carrier concentration. Unfortunately, most of epitaxial ZnO and related compound semiconductors belong to nanostructures in nature having incoherent grain boundaries, such as a nanowire, nanorod, nanowall, or nanobelt. Epilayer growth process of device quality ZnO was limited success even after many years of research. A major problem encountered in the single-crystal approach is routinely grown on the highly mismatched heteropitaxial substrates, such as Si, sapphire, and glass substrates [1-3]. The fabrication of $Zn_{1-x}(Be,Mg,Al)_xO$ makes it possible to de-couple strain and band gap engineering to achieve unique device structures that lead to novel photonic devices based on Group II-VI materials [4-11]. These systems include strain-engineered direct gap diodes and multi-quantum well lasers, photodetectors, emitters and modulators grown on $Zn_{1-x}(Be,Mg,Al)_xO$ buffered sapphire or virtual substrates.

To expand our insight into the stress/strain distributions in and around coherently strained ZnO-based group-II-VI $Zn_{1-x}(Be,Mg,Al)_xO$ alloy systems we performed ab initio calculations to elucidate the epitaxial stabilization. Our calculations using density functional theory (DFT) methods based on the generalized gradient approximation (GGA) proceed as follows. First of all, we construct $Zn_{1-x}(Be,Mg,Al)_xO$ strained layer models, and their atomic structures are optimized by full relaxation to zero force positions. Second, we calculate the epitaxial softening of (0001)-oriented $Zn_{1-x}(Be,Mg,Al)_xO$ models. Third, we calculate the epitaxial softening of (0001)-, $(10\bar{1}0)$-, and $(2\bar{1}\bar{1}0)$-oriented ZnO strained layer superlattices. Finally, we employ the harmonic elasticity theory to study the harmonic behavior of the $Zn_{1-x}(Be,Mg,Al)_xO$. Above calculations enable us to determine the preferred growth direction, the effect of dopant constituents on the epitaxial stabilization of the $Zn_{1-x}(Be,Mg,Al)_xO$ alloy systems, and the compressive or tensile relaxation in and around strained $Zn_{1-x}(Be,Mg,Al)_xO$ alloy systems.

II. COMPUTATIONAL METHODOLOGY AND BACKGROUND

A fundamental quantity which influences the epitaxial deformation behavior of thin films is the epitaxial stabilization (also commonly referred to as the epitaxial softening) which is defined as the ratio between the epitaxial increase in energy ΔE^{epi} due to bi-axial deformation, and the hydrostatic increase in energy ΔE^{bulk} due to tri-axial deformation. Formally, the epitaxial stabilization is defined by the dimensionless parameter [12]:

$$q(a,\hat{G}) = \Delta E^{epi}(a,\hat{G}) / \Delta E^{bulk}(a). \quad (1)$$

Here $\hat{G}$ is the growth direction and a is the in-plane lattice constant.

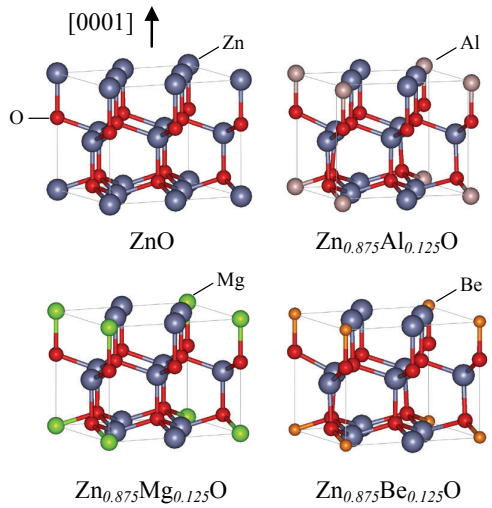

FIG. 1. Atomistic representations of ZnO, $Zn_{0.875}Al_{0.125}O$, $Zn_{0.875}Mg_{0.125}O$, and $Zn_{0.875}Be_{0.125}O$ models. The atoms are represented by spheres: Zn (light gray), O (red), Al (pink), Mg (light green) and Be (orange).

The epitaxial stabilization of the (0001)-oriented $Zn_{1-x}(Be,Mg,Al)_xO$ strained layer superlattices was studied in detail by conducting first-principles DFT-GGA calculations using the Vienna Ab Initio Simulation Package (VASP) [13], which utilizes a plane wave basis to solve the electronic structure. We employ ultrasoft pseudopotentials [14] and a plane-wave basis to treat the electronic structure within the PW 91 GGA [15,16]. We took into account 16-atom crystallographic unit cells with the compositions of ZnO, $Zn_{0.875}Be_{0.125}O$, $Zn_{0.875}Mg_{0.125}O$, and $Zn_{0.875}Al_{0.125}O$. All atomic positions were optimized by full relaxation to zero force positions. The convergence of electronic properties was achieved with a kinetic energy cutoff of 396 eV and 18 irreducible k-points generated within the Brillouin zone (BZ), yielding the optimized structures shown in the four models depicted in Fig. 1.

To investigate the systematic change in the preferred growth directions of ZnO systems, we examined (0001)-, $(10\bar{1}0)$-, and $(2\bar{1}\bar{1}0)$-oriented ZnO strained layer superlattices using the same computational parameters, i.e., a kinetic energy cutoff of 396 eV and 18 irreducible k points. The three

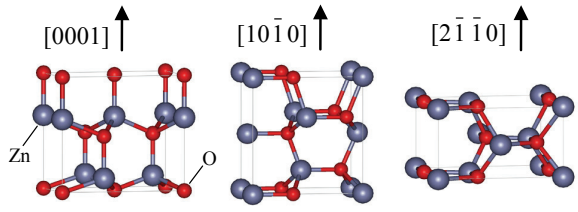

FIG.2. Schematic illustration of (0001)-, $(10\bar{1}0)$-, and $(2\bar{1}\bar{1}0)$-oriented ZnO strained layer superlattices

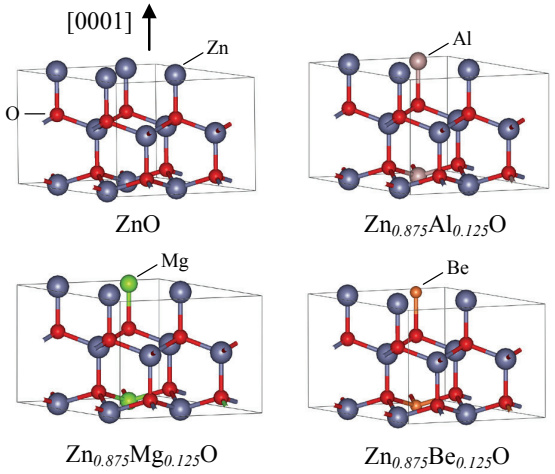

FIG. 3. Ball and stick structural representations of the four $Zn_{1-x}(Be,Mg,Al)_xO$ strained layer models considered in this study

models treated in the present work are optimized and described in Fig. 2.

$Zn_{1-x}(Be,Mg,Al)_xO$ are hexagonal crystals with six independent elastic stiffnesses C_{11}, C_{33}, C_{44}, C_{66}, C_{12}, and C_{13}. These elastic stiffnesses can be calculated through polynomial fitting to an energy-strain relation for the hexagonal crystals deformed using an appropriate strain tensor and carried out using the CAmbridge Serial Total Energy Package (CASTEP) [17]. Thus, to calculate the elastic stiffnesses of $Zn_{1-x}(Be,Mg,Al)_xO$ systems we adopt the $Zn_{1-x}(Be,Mg,Al)_xO$ crystallographic unit cell containing 8 formula unit (f.u.) of ZnO. The supercell consists of a 2×2×1 basic hexagonal primitive cell, which atomic positions were optimized by full relaxation to zero force positions as shown in Fig. 3. A 4×4×3 Monkhorst Pack (MP) grid in the first BZ and a kinetic energy cutoff of 300 eV were chosen to yield converged elastic stiffnesses through strain-stress theory implemented in the CASTEP.

III. RESULTS AND DISCUSSIONS

Epitaxial models with a variable and controllable range of compositions were constructed by using bulk crystalline configurations. The bulk strain energy is due to the (tri-axial) hydrostatically deformation and the epitaxial strain energy is due to the (bi-axial) epitaxially deformation. The bulk and epitaxial strain energies of all models are compared. Fig. 4 shows $q(a,[0001])$ in ZnO, $Zn_{0.875}Be_{0.125}O$, $Zn_{0.875}Mg_{0.125}O$, and $Zn_{0.875}Al_{0.125}O$ strained layer lattices over the wide strain range from -2% to 2%, indicating that hexagonal $Zn_{0.875}Al_{0.125}O$ is significantly softer than others in a film state. It is apparent that ZnO-based group-II-VI $Zn_{1-x}(Be,Mg,Al)_xO$ alloy systems become stiffer upon dilation (tensile strain). Our findings also indicate that the ZnO strained layers could be stabilized with adding the aluminum composition, which Al

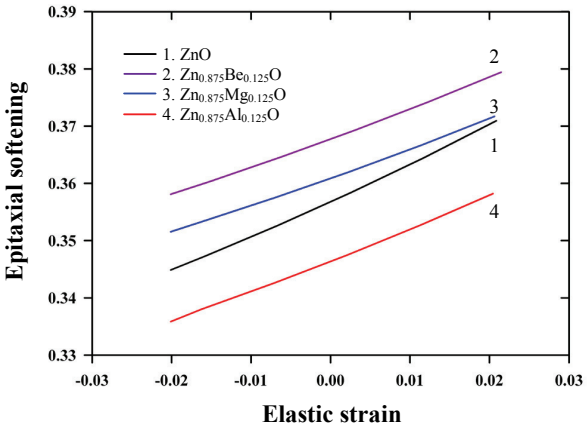

FIG. 4. $q(a_f,\hat{G})$ *vs* the elastic strain for (0001)-oriented ZnO (line 1), $Zn_{0.875}Be_{0.125}O$ (line 2), $Zn_{0.875}Mg_{0.125}O$ (line 3), and $Zn_{0.875}Al_{0.125}O$ (line 4) strained layer lattices.

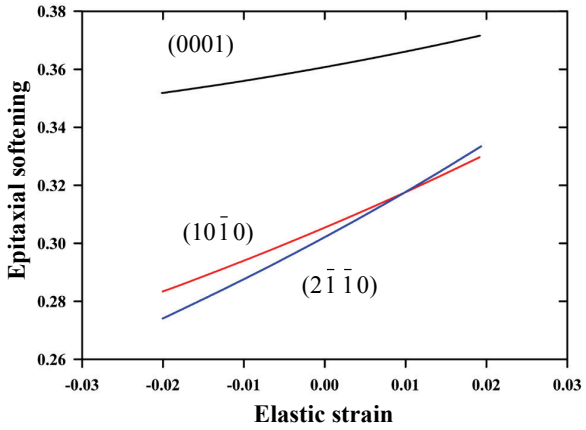

FIG. 5. The calculated epitaxial softening functions $q(a,\hat{G})$ versus epitaxial strain for (0001)-, (10$\bar{1}$0)- and (2$\bar{1}\bar{1}$0)-oriented ZnO.

is at substitutional sites in the underlying Zn lattice.

Furthermore, we are going to analyze the epitaxial softening of (0001)-, (10$\bar{1}$0)-, and (2$\bar{1}\bar{1}$0)-oriented ZnO strained layer superlattices for providing further insight into the stress/strain distributions in and around coherently strained ZnO-based systems. The results presented in Figure 5 show the elastically softest direction is <2$\bar{1}\bar{1}$0> and the hardest direction is <0001>. The results of our calculations are consistent with reported experimental observations that <2$\bar{1}\bar{1}$0>-oriented ZnO is more stable than (0001)- or (10$\bar{1}$0)-oriented ZnO [18].

To further elucidate the behavior of longitudinal and shear modes under pressure we report the elastic constants (C_{11}, C_{33}, C_{44}, C_{66}, C_{12}, and C_{13}) obtained by calculating the change in energy with strain for six different strain configurations, as shown in Table 1. The pronounced softening of the longitudinal modulus C_{11} and C_{33} is found with adding the aluminum composition to ZnO. In addition, the table lists the bulk modulus K calculated from the fitting of total energy versus volume to the equation of state of a third-order Birch-Murnaghan. The relation $K=2/9\,(C_{11}+C_{12}+2C_{13}+0.5C_{33})$ provides a useful internal consistency check for calculated elastic stiffnesses. Using the C_{66}/C_{44} ratio as a shear-mode elastic anisotropy criterion, we found that the ZnO and $Zn_{0.875}Al_{0.125}O$ have the weak elastic anisotropy (or isotropic elastic properties). The dopant compositions such as elemental Be and Mg have a direct influence on the elastic anisotropy.

The harmonic behavior of the $Zn_{1-x}(Be,Mg,Al)_xO$ is not well known. For solving this mystery, we employ the hexagonal harmonics elasticity theory [19]. As shown in Fig. 6, the $q_{harm}([0001])$ is the highest and the $q_{harm}([2\bar{1}\bar{1}0])$ is much softer than <0001> or <10$\bar{1}$0>. Apart from <2$\bar{1}\bar{1}$0>, the $q_{harm}([11\ \bar{2}\ l])$ is the only other smaller value in $Zn_{1-x}(Be,Mg,Al)_xO$ layer lattices, where l is an arbitrary value. Our result is consistent with the experimental observations that the (11$\bar{2}$3) faces of three-dimensional ZnO pyramids grow faster than (0001) and (10$\bar{1}$0) faces [20].

IV. CONCLUSIONS

The epitaxial softening of $Zn_{1-x}(Be,Mg,Al)_xO$ strained layer lattices was studied by first-principles DFT-GGA calculations. We found that the ZnO strained layers could be stabilized with adding the aluminum composition. Dopant compositions such as elemental Be and Mg have a direct

TABLE 1. Summary of calculated elastic module for ZnO, $Zn_{0.875}Al_{0.125}O$, $Zn_{0.875}Mg_{0.125}O$, and $Zn_{0.875}Be_{0.125}O$.

	C_{11} (GPa)	C_{33} (GPa)	C_{44} (GPa)	C_{66} (GPa)	C_{12} (GPa)	C_{13} (GPa)	K (GPa)	C_{66}/C_{44}
ZnO	174.90	186.55	40.89	38.96	75.10	62.96	105.69	0.95
$Zn_{0.875}Al_{0.125}O$	168.85	173.13	37.32	37.37	75.36	62.02	98.27	1.00
$Zn_{0.875}Mg_{0.125}O$	186.20	192.15	36.63	51.48	88.09	72.28	110.41	1.41
$Zn_{0.875}Be_{0.125}O$	156.69	198.72	34.06	47.09	69.90	48.75	92.46	1.38

influence on the elastic anisotropy. The elastically softest direction is <2 $\bar{1}$ $\bar{1}$ 0> and the hardest direction is <0001>. According to the harmonic elasticity theory, the <11 $\bar{2}$ *l*> direction such as <11 $\bar{2}$ 3> is the other soft direction in $Zn_{1-x}(Be,Mg,Al)_xO$ layer lattices

ACKNOWLEDGMENTS

This work was supported by the National Science Council under Contract No. NSC98-2112-M-005-005-MY3, by the Ministry of Economic Affairs, Taiwan, Republic of China with Grant No. 97-EC-17-A-07-S1-097, and in part by the Ministry of Education, Taiwan, R.O.C. under the ATU plan. Computational studies were performed using the resources of the National Center for High-performance Computing.

REFERENCES

[1] Y. Chen, D. M. Bagnall, H. Koh, K. Park, K. Hiraga, Z. Zhu, and T. Yao, J. Appl. Phys. 84, 3912 (1998).
[2] W. Xu, Z. Ye, T. Zhou, B. Zhao, L. Zhu, and J. Huang, J. Cryst. Growth 265, 133 (2004).
[3] H. W. Lee, S. P. Lau , Y. G. Wang, B. K. Tay and H. H. Hng, Thin Solid Films 458, 15 (2004).
[4] A. Tsukazaki, A. Ohtomo, T. Onuma, M. Ohtani, T. Makino, M. Sumiya, K. Ohtani, S. F. Chichibu, S. Fuke, Y. Segawa, H. Ohno, H. Koinuma and M. Kawasaki, Nat. Mater. 4, 42 (2005).
[5] T. P. Smith, W. J. Mecouch, P. Q. Miraglia, A. M. Roskowski, P. J. Hartlieb, and R. F. Davis, J. Cryst. Growth 257, 255 (2003).
[6] H. Xu, K. Ohtani, M. Yamao, and H. Ohno, Appl. Phys. Lett. 89, 71918 (2006).
[7] K. Koike, K. Hama, I. Nakashima, S. Sasa, M. Inoue and M. Yano, Jpn. J. Appl. Phys. 44, 3822 (2005).
[8] H. Tampo, H. Shibata, K. Maejima, A. Yamada, K. Matsubara, P. Fons, S. Niki, T. Tainaka, Y. Chiba, and H. Kanie, Appl. Phys. Lett. 91, 261907 (2007).
[9] Y. R. Ryu, J. A. Lubguban, T. S. Lee, H. W. White, T. S. Jeong, C. J. Youn, and B. J. Kim, Appl. Phys. Lett. 90, 131115 (2007).
[10] Y. Ryu, T. S. Lee, J. A. Lubguban, H. W. White, B. J. Kim, Y. S. Park, and C. J. Youn, Appl. Phys. Lett. 88, 241108 (2006).
[11] Y. Luo, J. Bian, J. Sun, H. Liang, and W. Liu, J. Mater. Process. Technol. 189, 473 (2007).
[12] V. Ozolins, C. Wolverton, and A. Zunger, Appl. Phys. Lett. 72, 427 (1998).
[13] G. Kresse and J. Furthmüller, Phys. Rev. B 54, 11169 (1996); G. Kresse and J. Furthmüller, Comput. Mater. Sci. 6, 15 (1996); G. Kresse and J. Hafner, J. Phys. Condens. Matter 6, 8245 (1994); G. Kresse and J. Joubert, Phys. Rev. B 59, 1758 (1999).
[14] D. Vanderbilt, Phys. Rev. B 41, 7892 (1990).
[15] J. P. Perdew and Y. Wang, Phys. Rev. B 45, 13244 (1992).

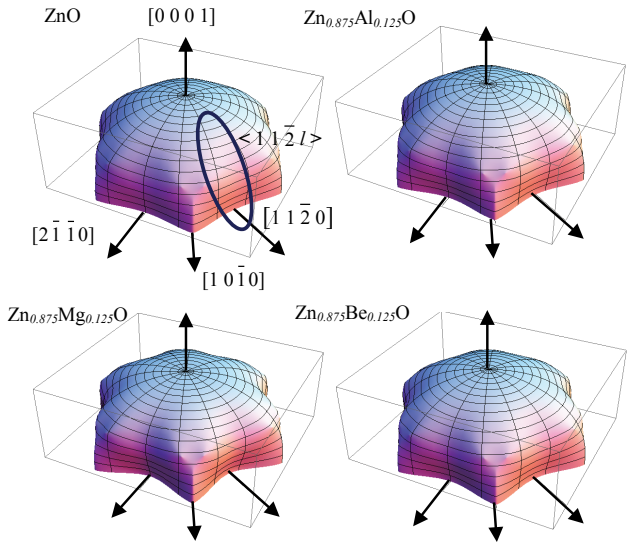

FIG. 6. 3D plot of epitaxial softening q_{harm} of the four $Zn_{1-x}(Be,Mg,Al)_xO$ strained layer models.

[16] J. P. Perdew, J. A. Chevary, S. H. Vosko. K. A. Jackson, M. R. Petersen, and C. Fiolhais, Phys. Rev. B 46, 6671 (1992).
[17] M. C. Payne, M. P. Teter, D. C. Allan, T. A. Arials, and J. D. Joannopoulos. Rev. Mod. Phys. 64, 1045 (1992); V. Milman, B. Winkler, J. A. White, C. J. Pickard, M. C. Payne, E. V. Akhmatskaya, and R. H. Nobes, Int. J. Quantum Chem. 77, 895 (2000).
[18] X. Y. Kong and Z. L. Wang, Nano Lett. 3, 1625, (2003).
[19] V. Ozoliņš, C. Wolverton, and Alex Zunger, Appl. Phys. Lett. 72, 427 (1998).
[20] J. B. Baxter, F. Wu, and E. S. Aydil, Appl. Phys. Lett. 83, 3797 (2003).